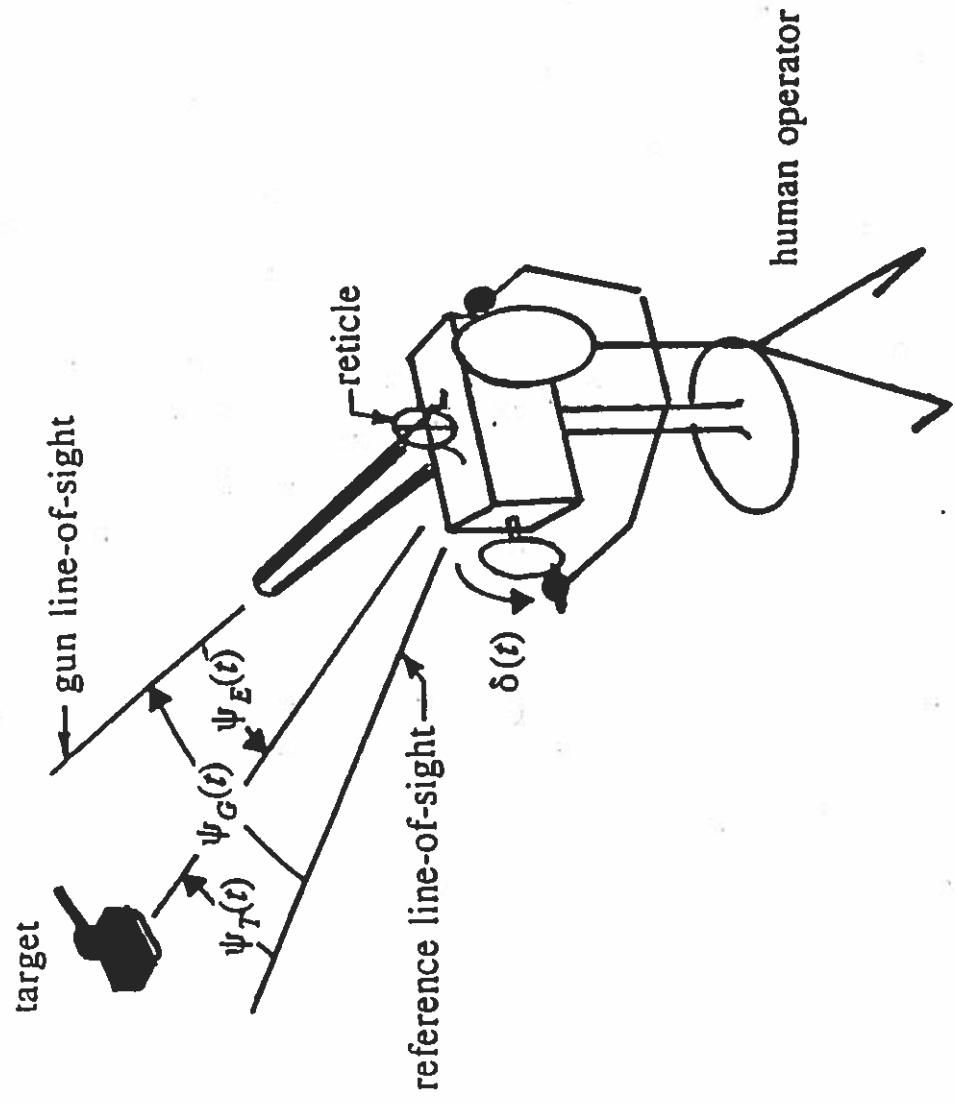


Human-in-the-Loop Control

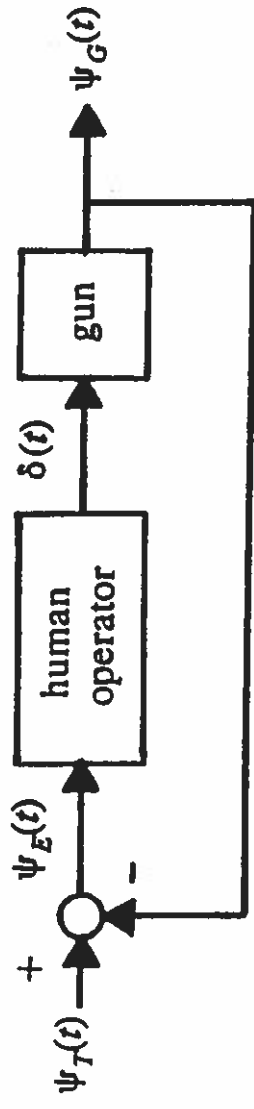
Ronald A. Hess

Dept. of Mechanical and Aeronautical Engineering
University of California
Davis, CA

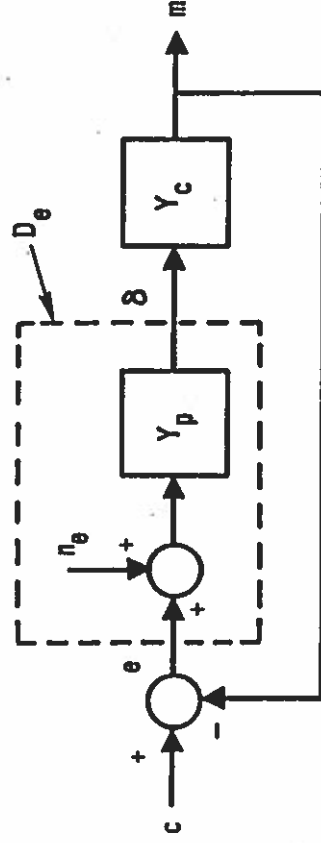
A Manual Control Task



Block Diagram Representation of the Gunnery Task



Determining the Human Operator "Transfer Function"



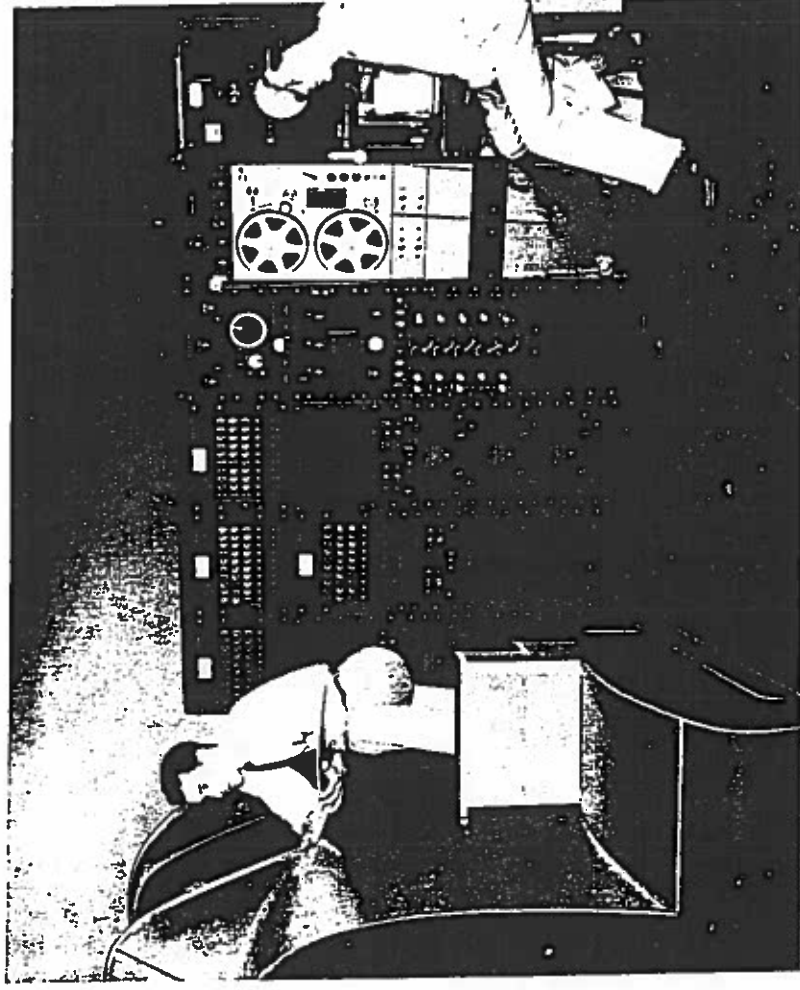
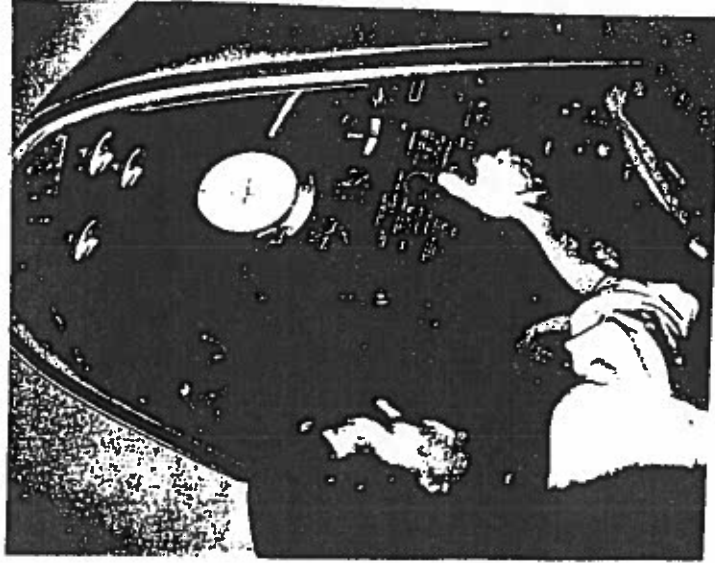
n_e = Operator Remnant

Y_p = Operator Transfer Function

$$Y_p(j\omega) = \frac{\Phi_{c\delta}(j\omega)}{\Phi_{ce}(j\omega)}$$

$$\Phi_{n n_e}(\omega) = \frac{|1 + Y_c Y_p(j\omega)|^2}{Y_p(j\omega)^2} \Phi_{\delta\delta}(\omega) - \Phi_{c c}(\omega)$$

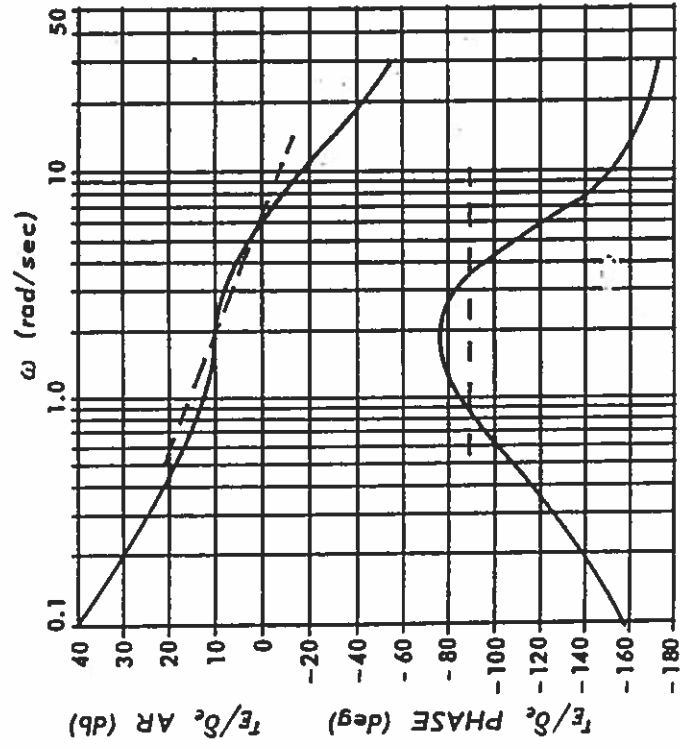
Determining the Human Operator "Transfer Function" The Early Experiments



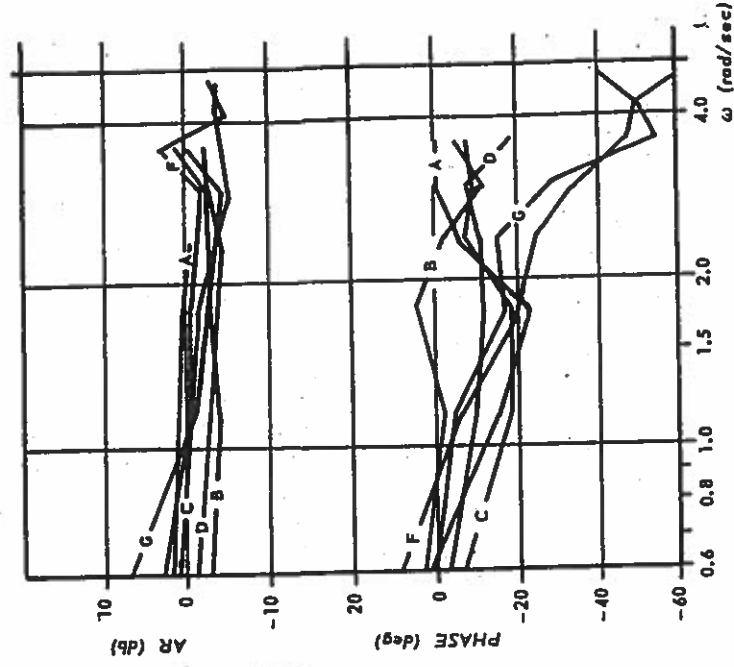
Cockpit and computer racks - Franklin Institute Simulator ~ 1952

Determining the Human Operator "Transfer Function" The Early Experiments

Franklin Institute Data



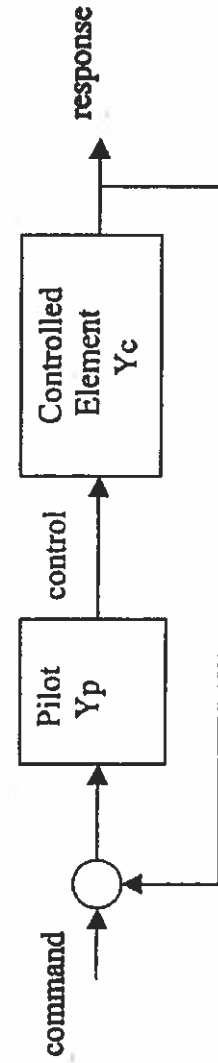
Vehicle dynamics



Pilot Dynamics

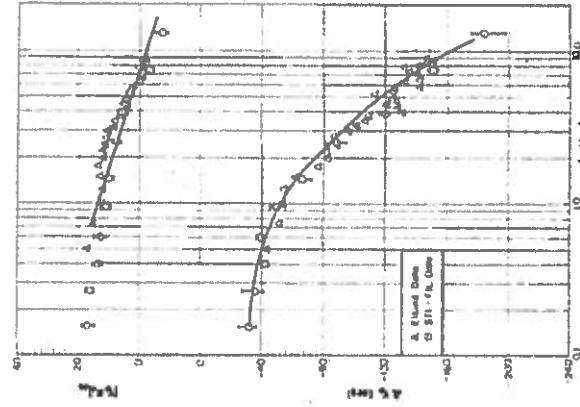
The Crossover Model of the Human Pilot

“McRuer’s Law”

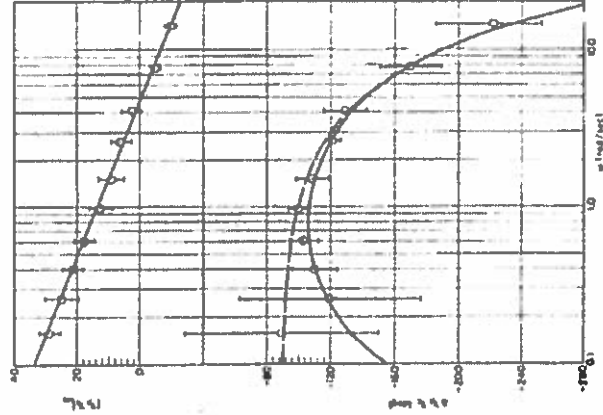


around open-loop crossover
frequency

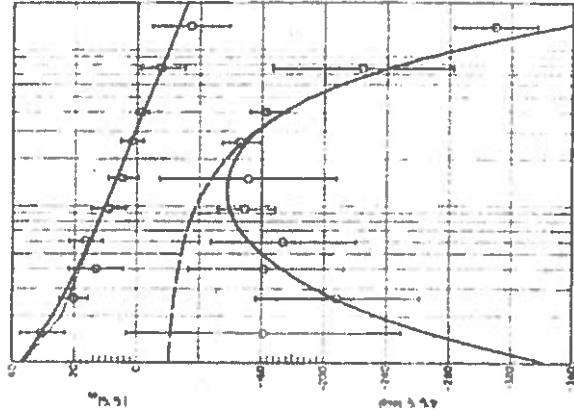
$$Y_p Y_c \approx \frac{\omega_c}{s} e^{-\tau s}$$



$$Y_c = K$$



$$Y_c = K/s$$

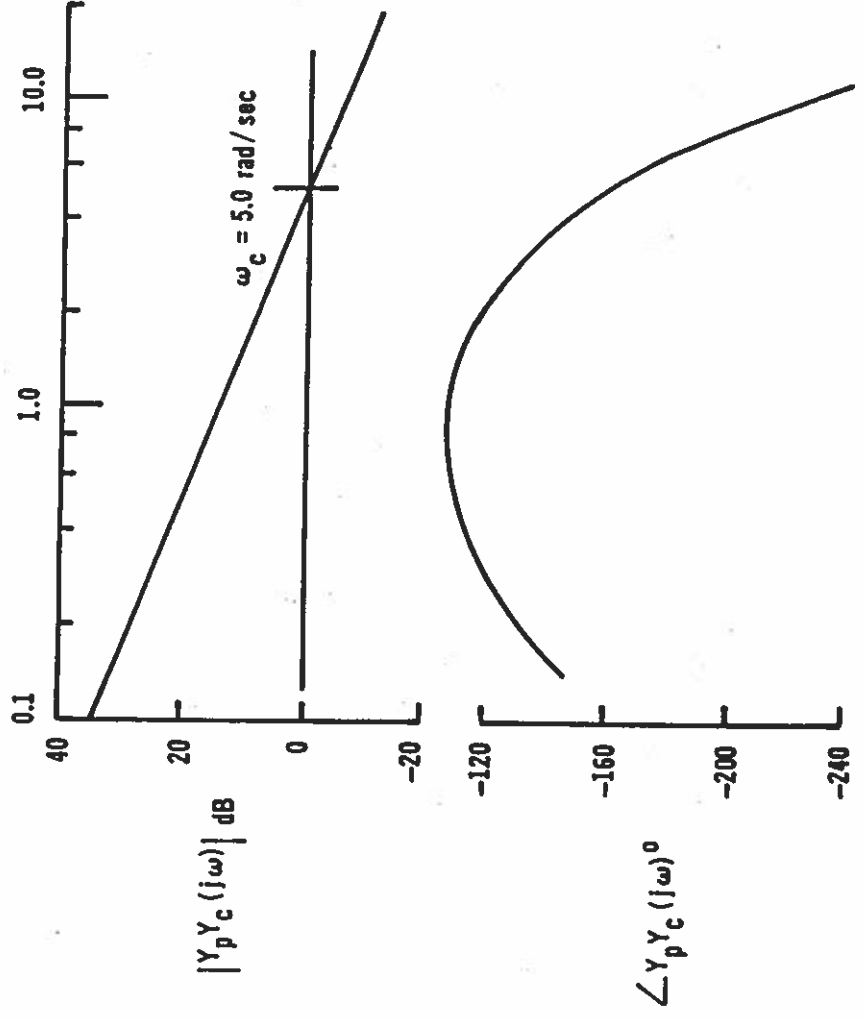


$$Y_c = K/s^2$$

The “Crossover Model” of the Human Operator

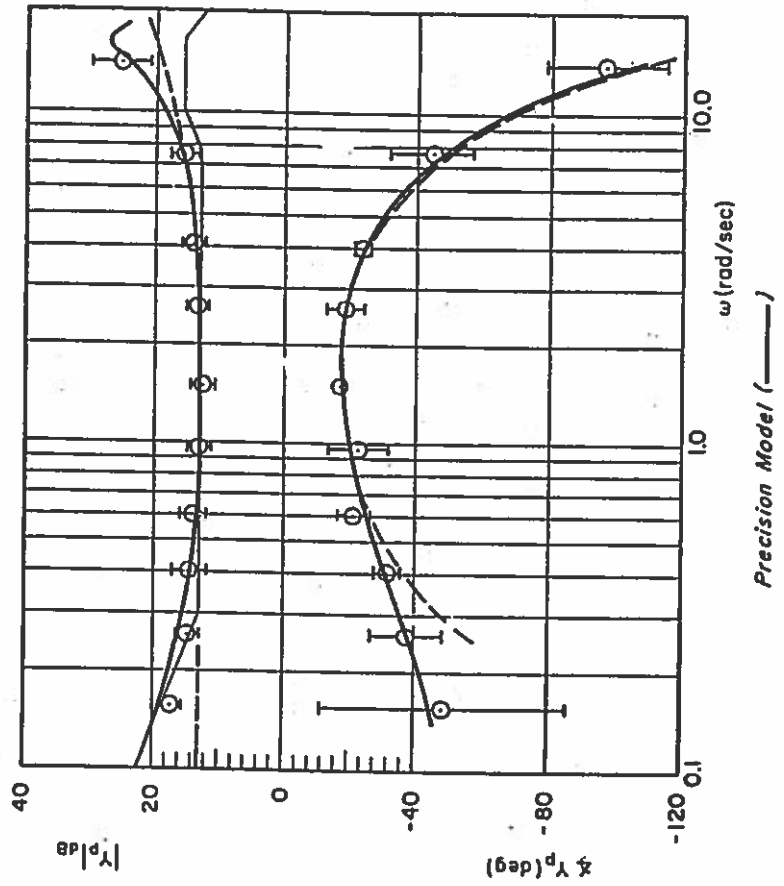
On basis of experiment, one could state with confidence, that in the region of open-loop crossover frequency,

$$Y_p Y_c \cong \omega_c e^{-\tau s} / s$$



The "Precision Model" of the Human Operator

$$Y_p(s) = K_p e^{-\tau s} \left(\frac{T_L s + 1}{T_I s + 1} \right) \left(\frac{T_K s + 1}{T'_K s + 1} \right) \left(\frac{1}{(T_{N_1} s + 1) \left[\left(\frac{s}{\omega_N} \right)^2 + \left(\frac{2\zeta_N}{\omega_N} \right) s + 1 \right]} \right)$$



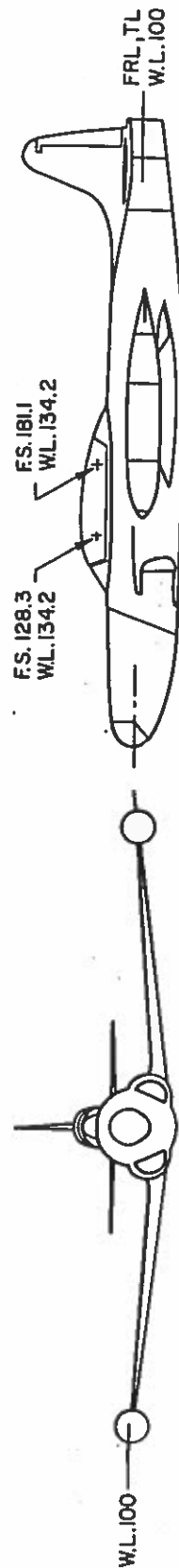
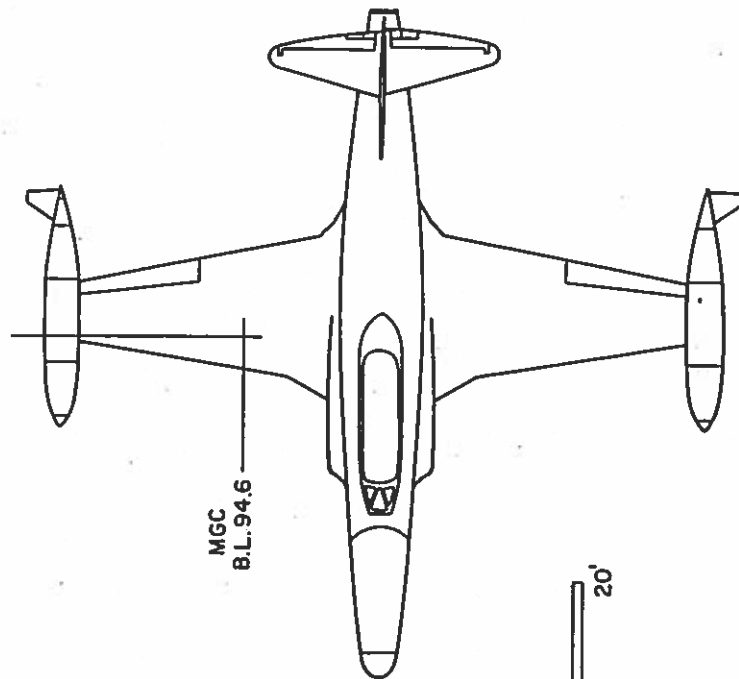
Variable Stability Research Aircraft USAF/CALSPAN NT-33A

NT-33A

$S = 234.8 \text{ ft}^2$

$b = 37.54 \text{ ft}$

$\bar{c} = 6.72 \text{ ft}$



In-Flight Measurements of the Human Transfer Function

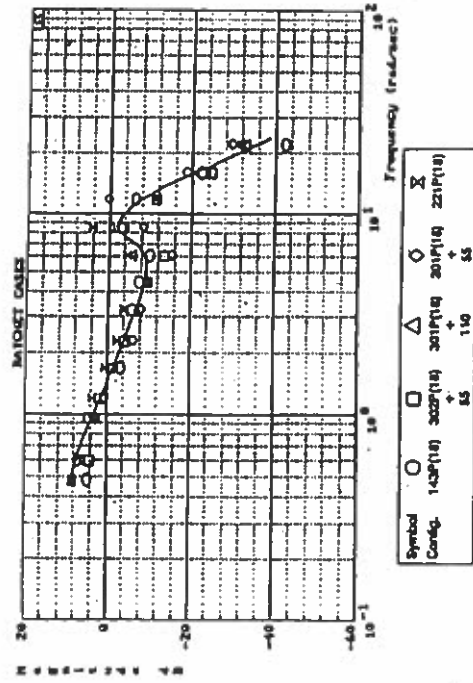


Figure 35. $Y_p Y_c$ Describing Functions for Ratchet Cases

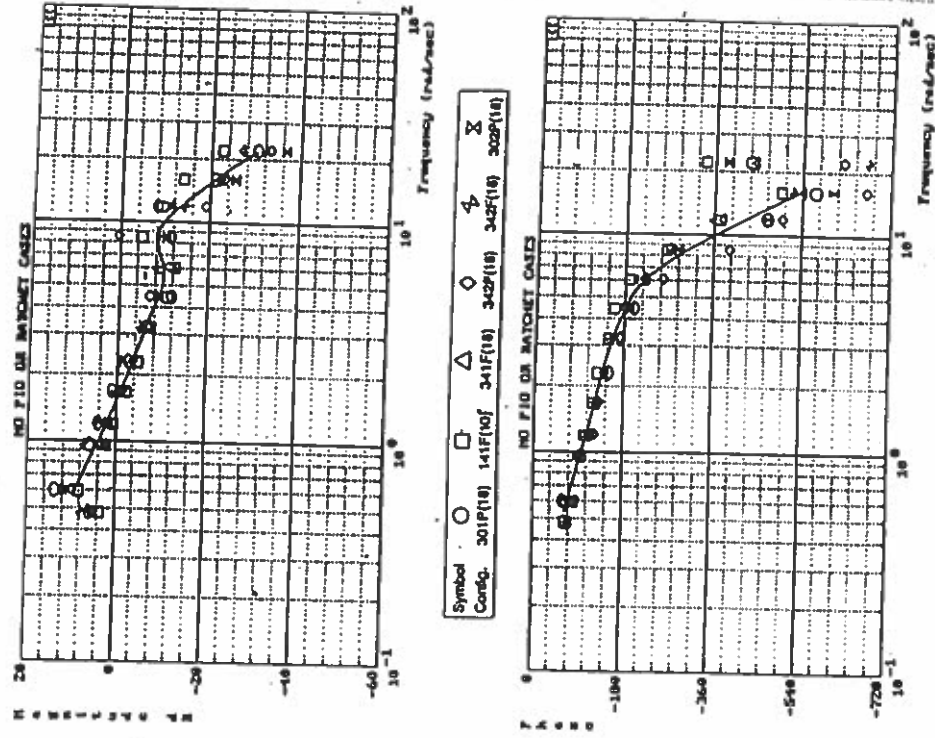
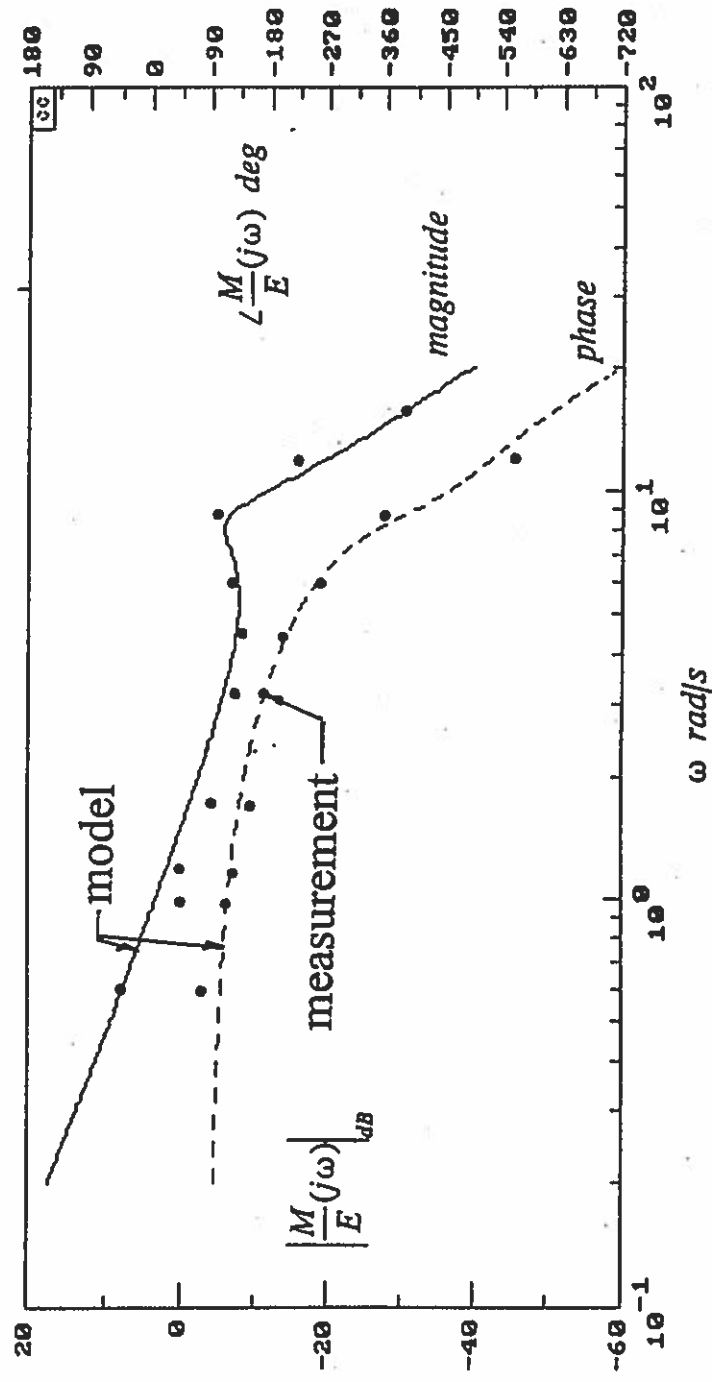


Figure 37. $Y_p Y_c$ Describing Functions for Level 1 Cases (No Ratchet or P10)

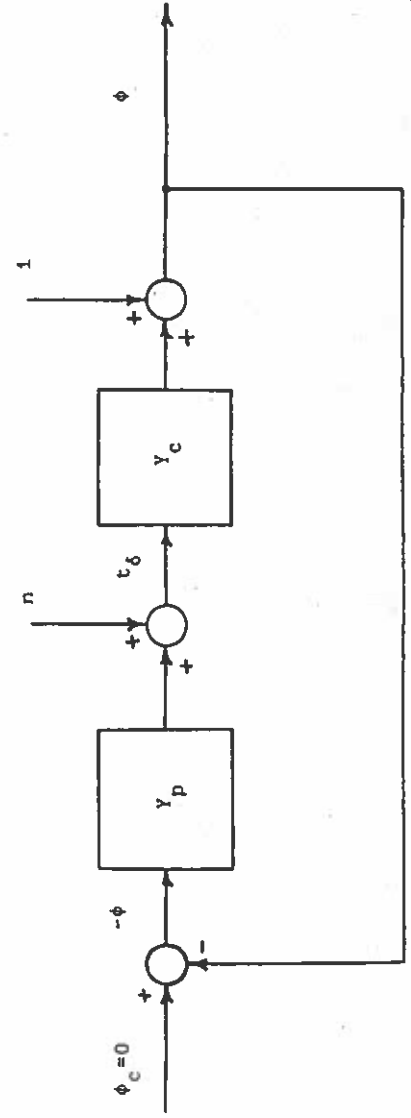
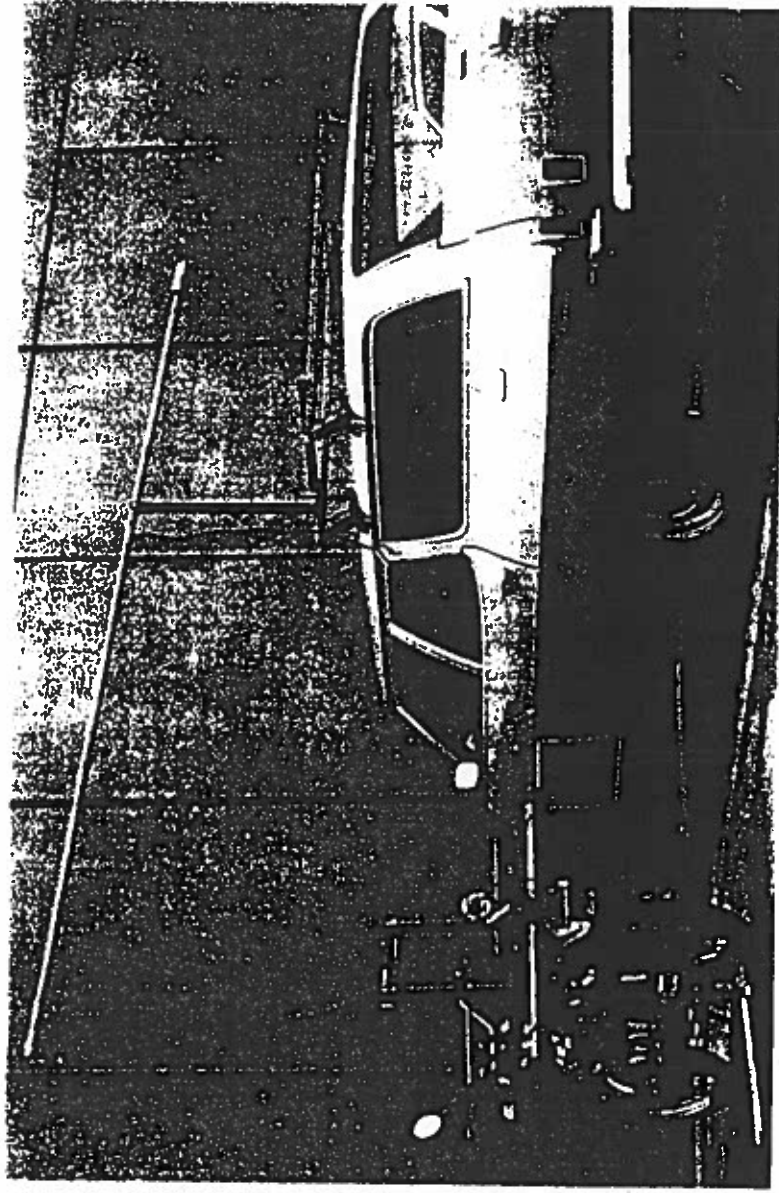
Mitchell, D. G., Aponso, B. L., and Klyde, D. H., "Effects of Cockpit Lateral Stick Characteristics on Handling Qualities and Pilot Dynamics, NASA CR 4443, June 1992.

Example of Model Comparison with In-flight Measurement of $Y_p Y_c$

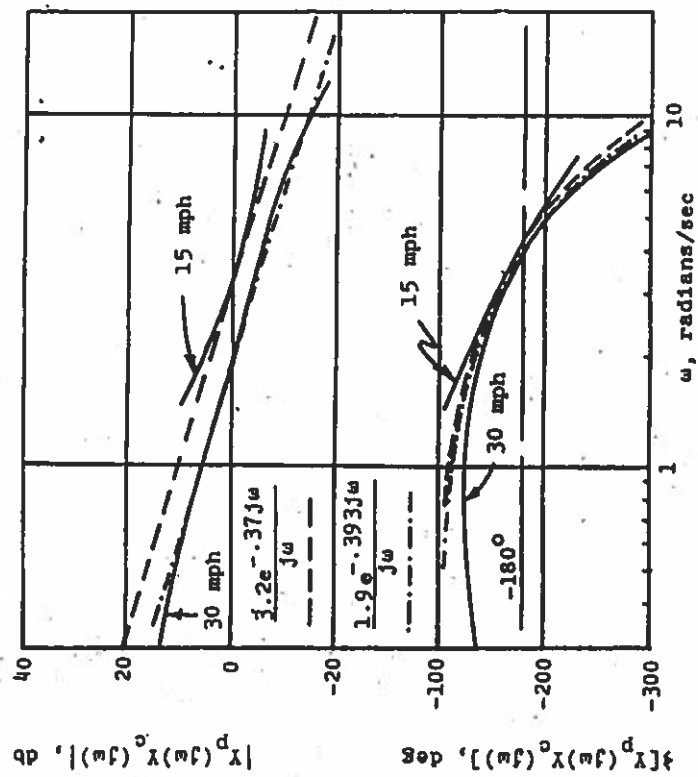
Comparison of pilot/vehicle transfer function from Structural Model with flight
test: Air Force CALSPAN NT33-A roll tracking task



The Transfer Function for the Motorcycle Rider in a Roll Stabilization Task



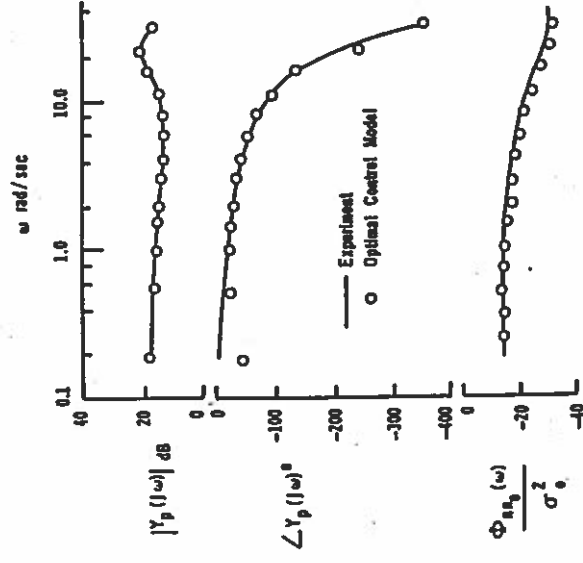
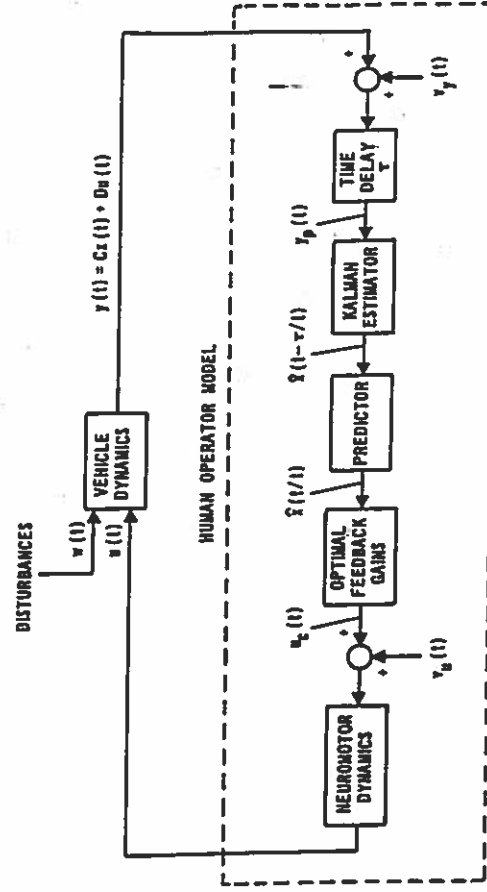
The Transfer Function for the Motorcycle Rider in a Roll Stabilization Task



$$Y_p(s) = 261e^{-0.3s} \left(\frac{s}{6.45} + 1 \right)$$

An "Algorithmic Model" of the Human Operator

The Optimal Control Model (OCM)



In-Flight Measurements of the Human Transfer Function

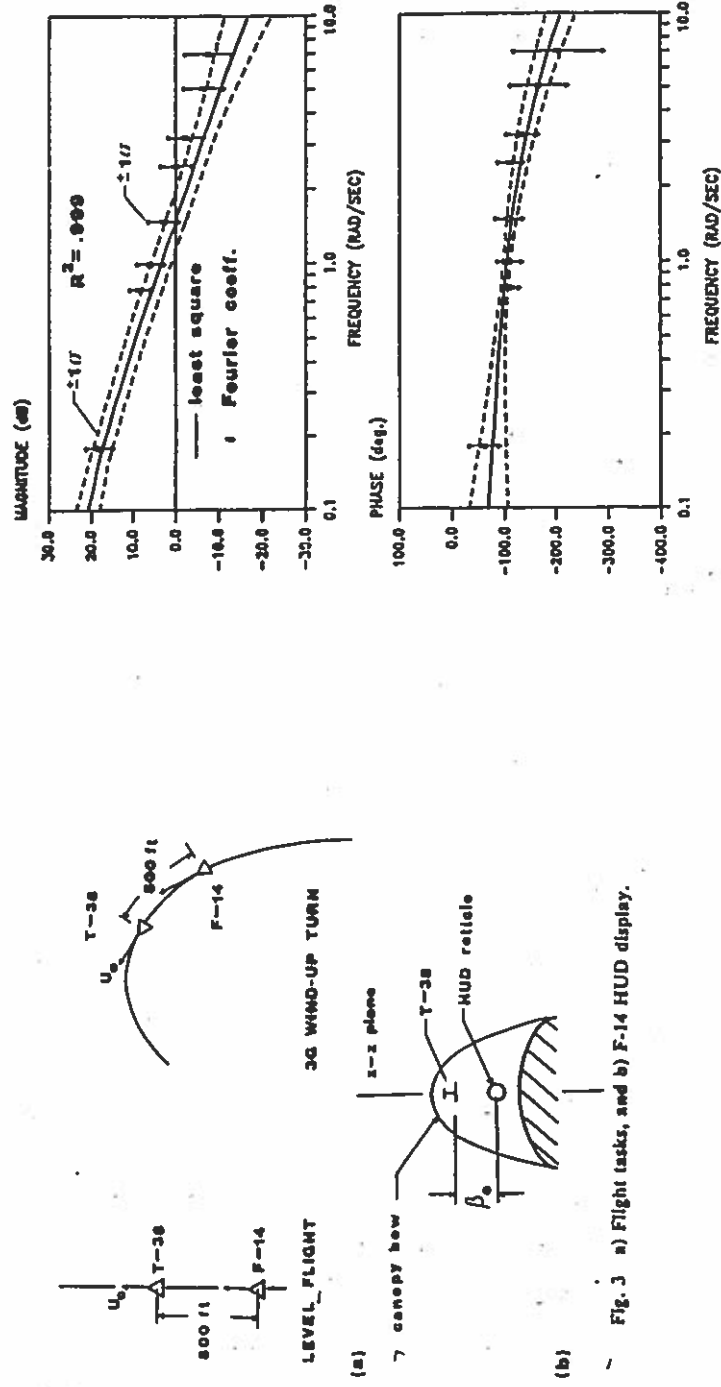


Fig. 3 a) Flight tasks, and b) F-14 HUD display.

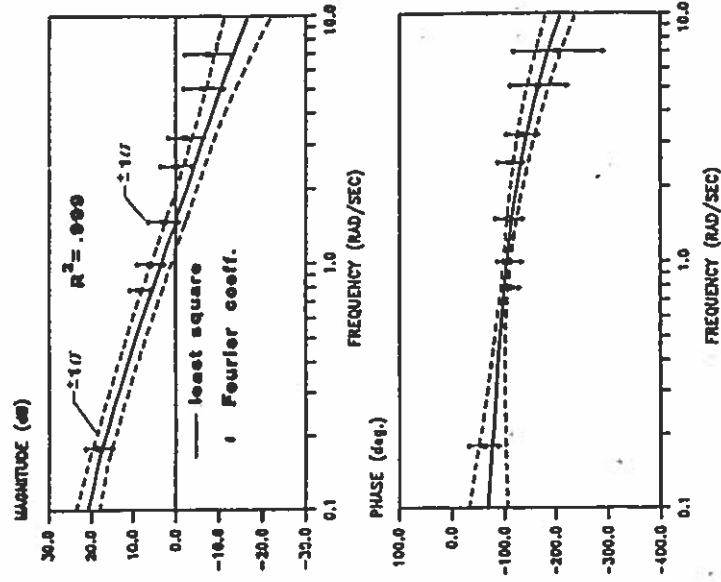


Fig. 11 Identification of F-14 pilot-vehicle system, 3-g turn, entry 5.

Hess, R. A., and Mnich, M. A. "Identification of Pilot-Vehicles Dynamics from In-Flight Tracking Data," *Journal of Guidance, Control, and Dynamics*, Vol. 9, No. 4, July-August, 1986, pp. 433-440.

Choosing the Crossover Frequency (The Last Step)

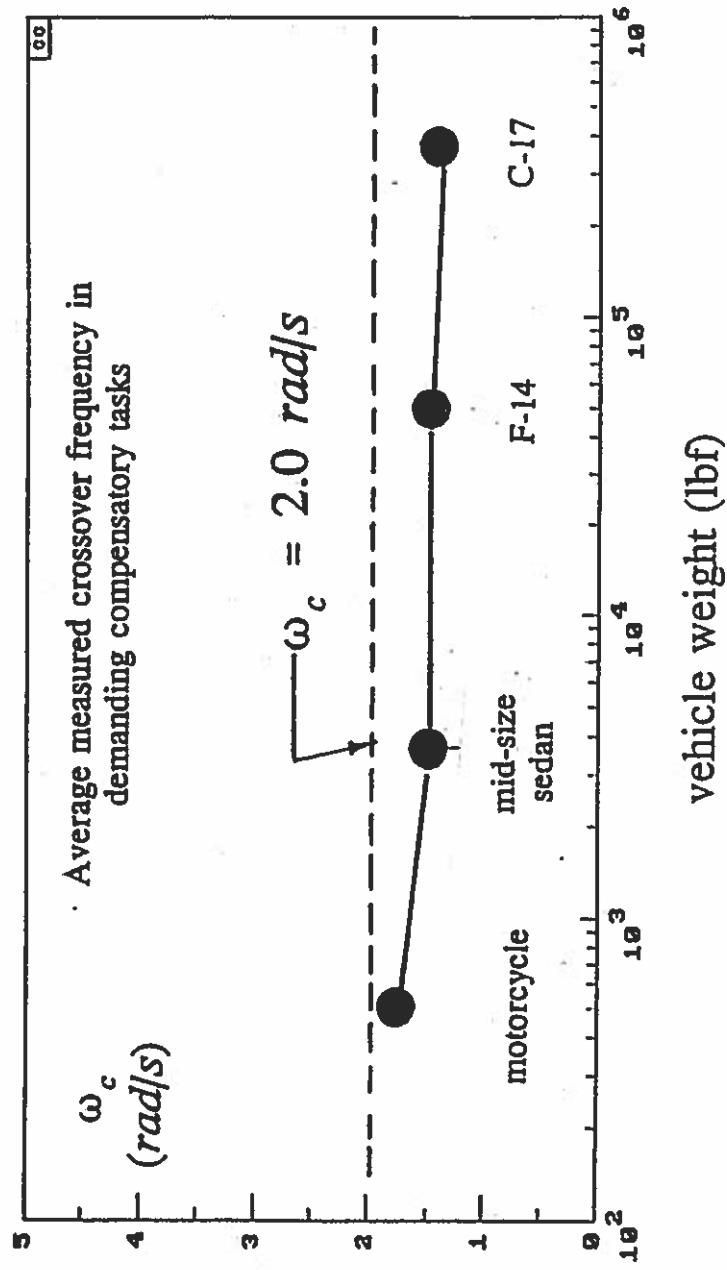
- Recalling the crossover model of the pilot,

$$Y_p Y_c(j\omega) = \frac{\delta_M}{E} (j\omega) \cdot Y_c(j\omega) \approx \frac{\omega_c}{j\omega} e^{-\tau_e s} \quad \text{for } \omega \approx \omega_c$$

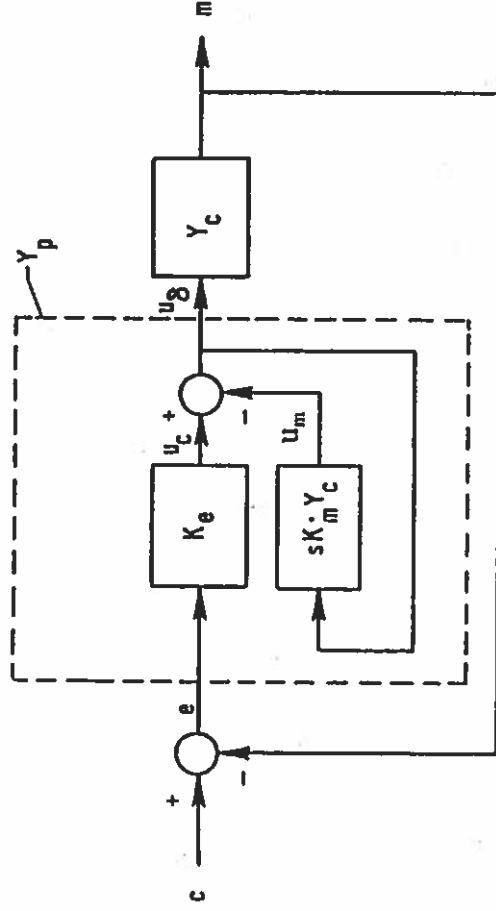
- For $\omega_c < 0.34/\tau_e$, closed-loop bandwidth becomes very sensitive to ω_c ; Using $\tau_e = 0.2$ sec, means a minimum acceptable ω_c would be

$$\omega_c \cong 0.34/0.2 \cong 2 \text{ rad/sec}$$

Crossover Frequency Invariant with Vehicle Size

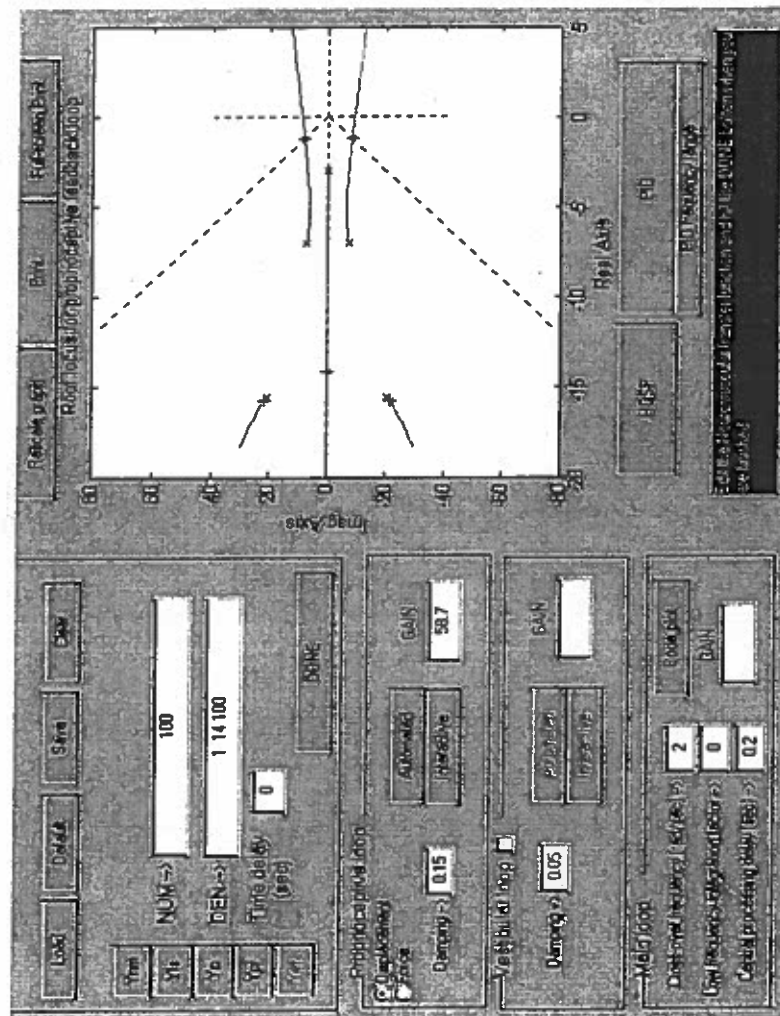


A Rudimentary “Structural Model” of the Human Operator

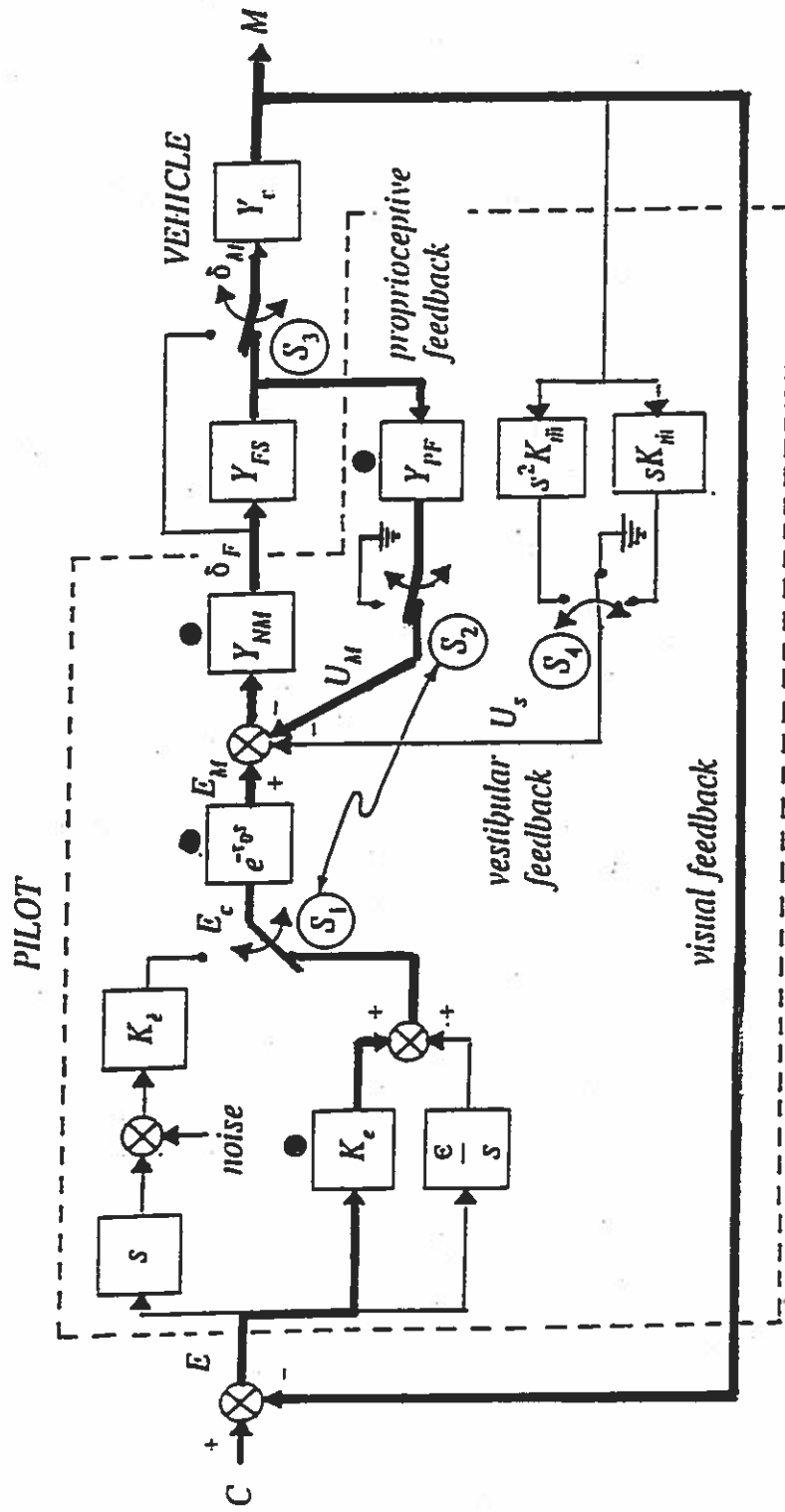


$$\left. \begin{aligned} Y_c &= K, & \frac{u_m}{u_\delta} &= (K_m K) s \\ Y_c &= \frac{K}{s}, & \frac{u_m}{u_\delta} &= K_m K \\ Y_c &= \frac{K}{s^2}, & \frac{u_m}{u_\delta} &= \frac{K_m K}{s} \end{aligned} \right\} Y_p Y_c \approx \frac{K_p}{s} e^{-\tau_e s}$$

Improved Version of PVD_{NL} with GUI



A More Complete Structural Model of the Human Operator

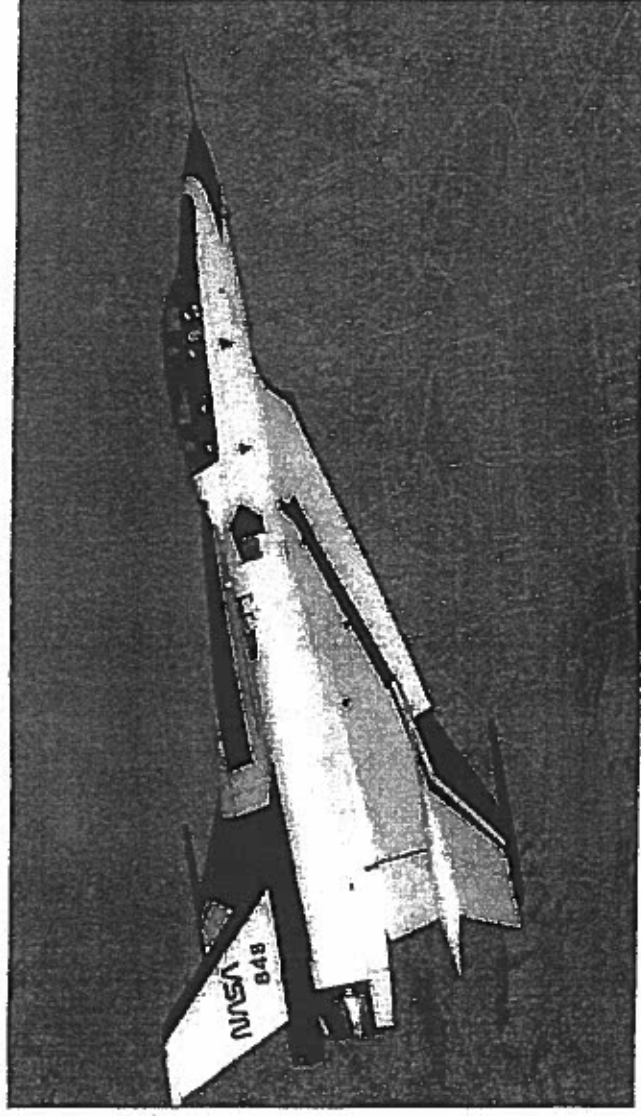


The Aircraft Roll-Ratchet Phenomenon

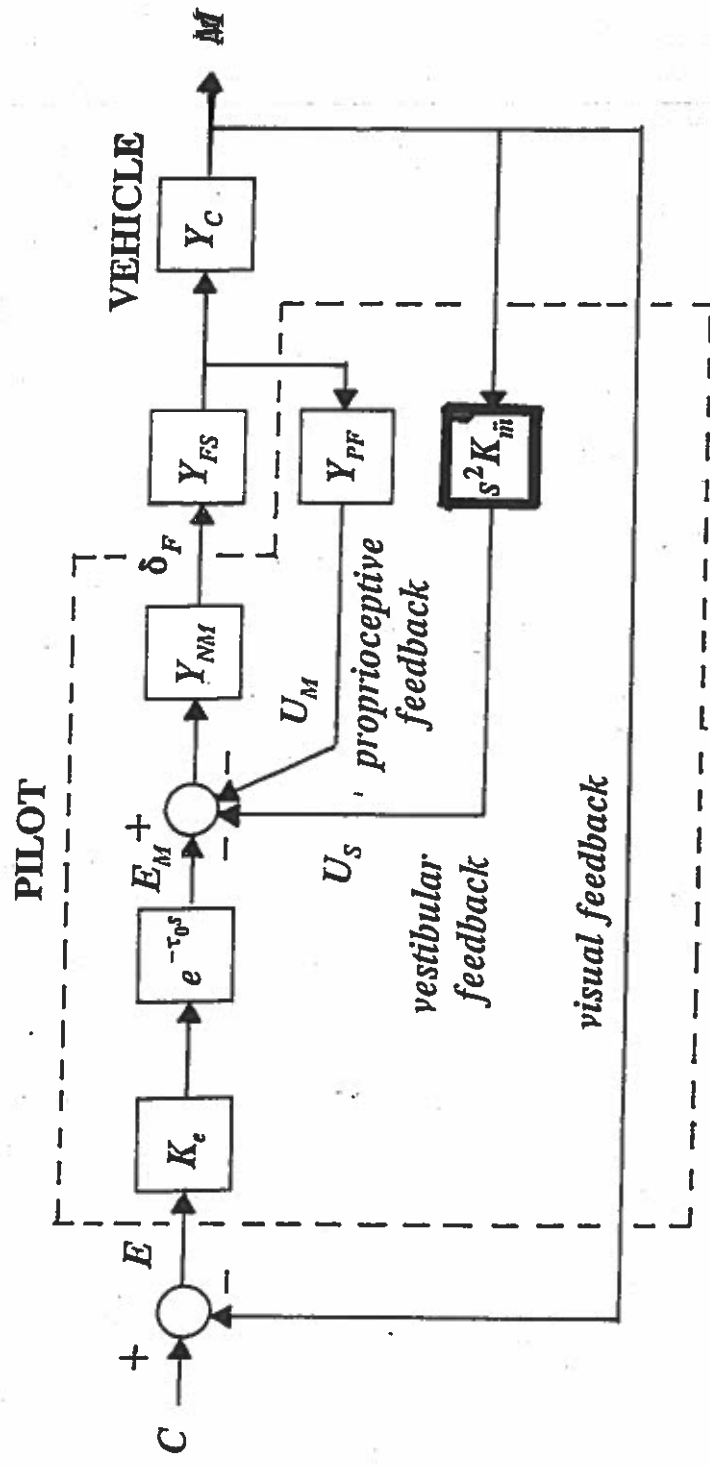
Latest documented occurrence: F-16XL, ship # 2

Serious roll-ratchet lasting approx. 4-5 sec

Pilot attempting to capture desired roll angle after three rapid 360 deg rolls



Exercising the Model Including Vestibular (Acceleration) Feedback



Exercising the Model

The Aircraft Roll-Ratchet Phenomenon

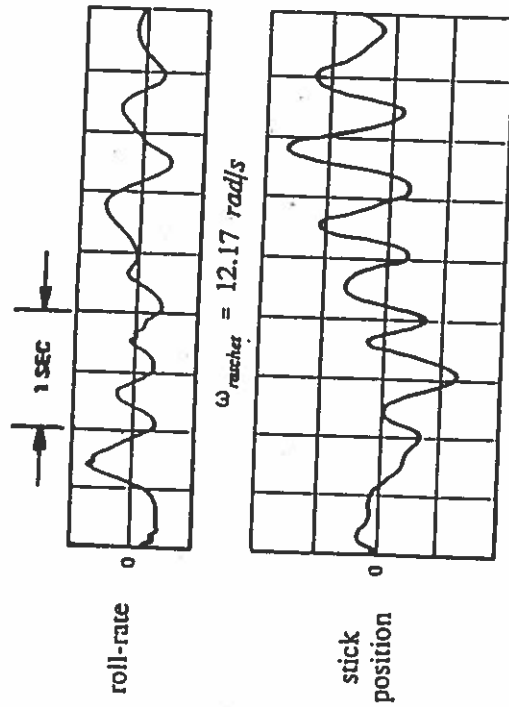
- Model-based hypothesis:
 - *pilot experiences roll accelerations which are deemed excessive - attempts to diminish these by feeding back acceleration sensed by vestibular system...however inappropriately large gain is used*
- Vestibular feedback employed in Structural Model
- Analysis conducted on 11 configurations flight tested on NT-33A aircraft...configurations differed in characteristics of force/feel system (e.g., whether flight control system commanded by inceptor position or applied force)

Exercising the Model

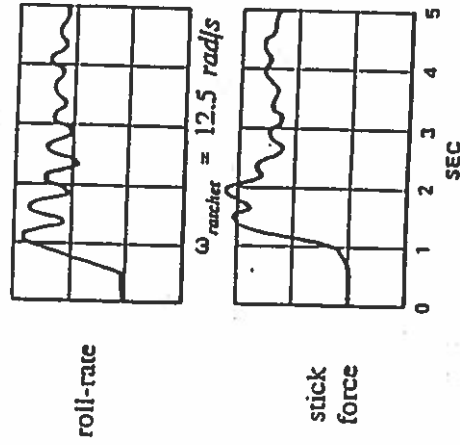
The Aircraft Roll-Ratchet Phenomenon

“Roll-ratchet defines a pilot-in-the-loop oscillation typically occurring in roll tracking of high-performance aircraft...frequency is considerably higher than “typical” pilot-induced oscillation, e.g. 2 Hz.

NT-33A

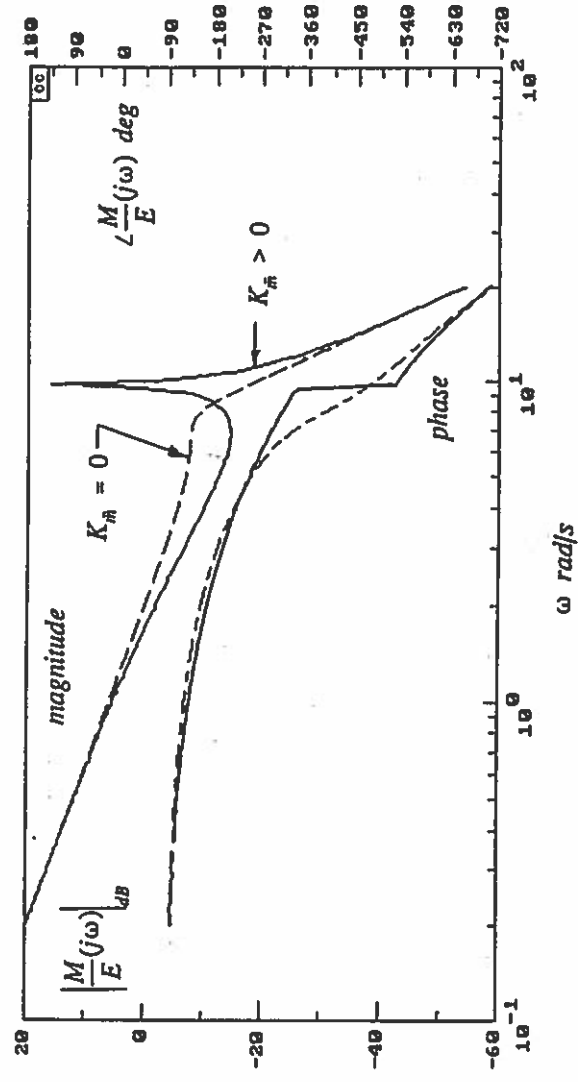


YF-16

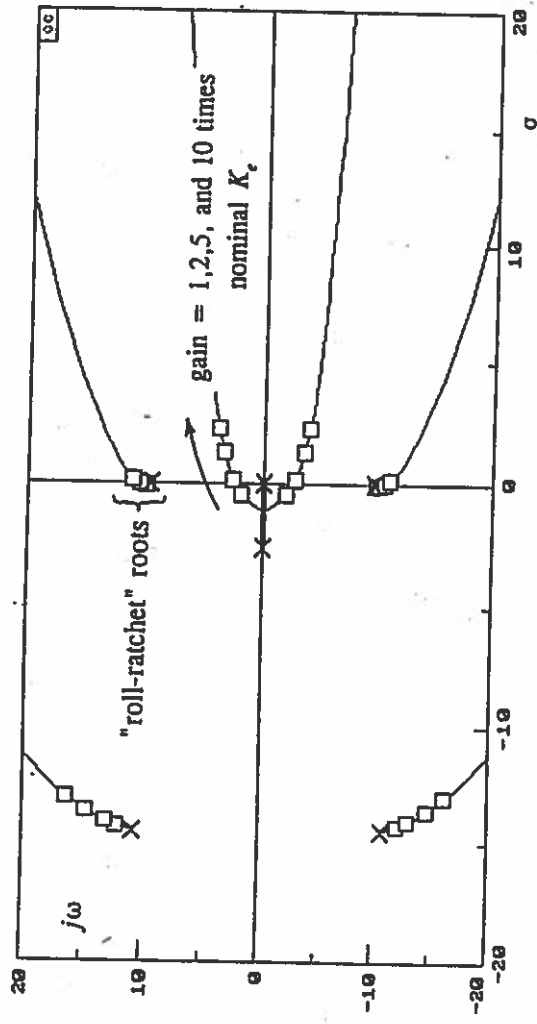


Increasing Vestibular Feedback Gain in Structural Model

Configuration 143P(18)

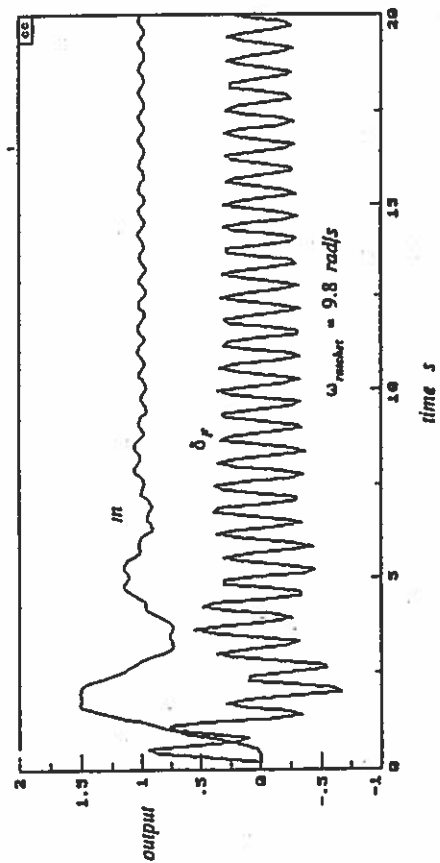
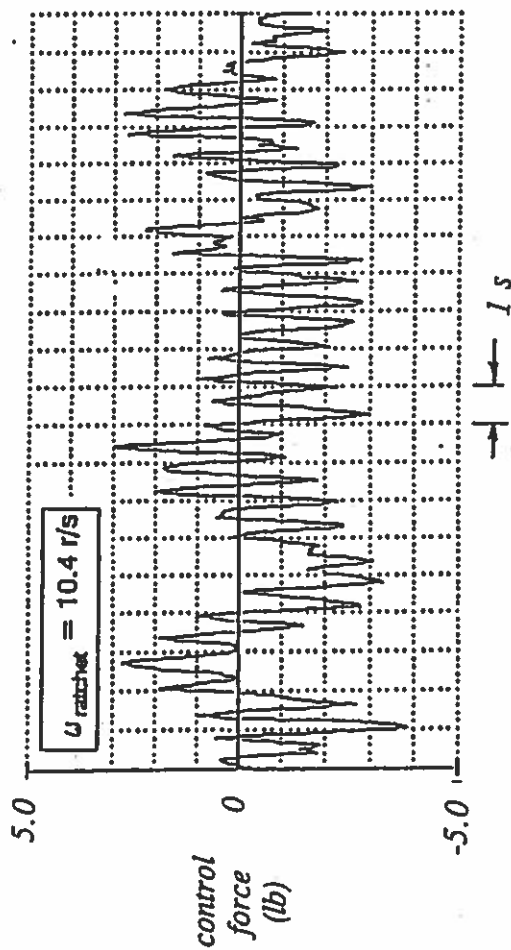


Ineffectiveness of Changing Visual Channel Gain to Halt Ratchet in Structural Model



Model and Flight Test Ratchet Time-History Comparison

Configuration 143P(18)

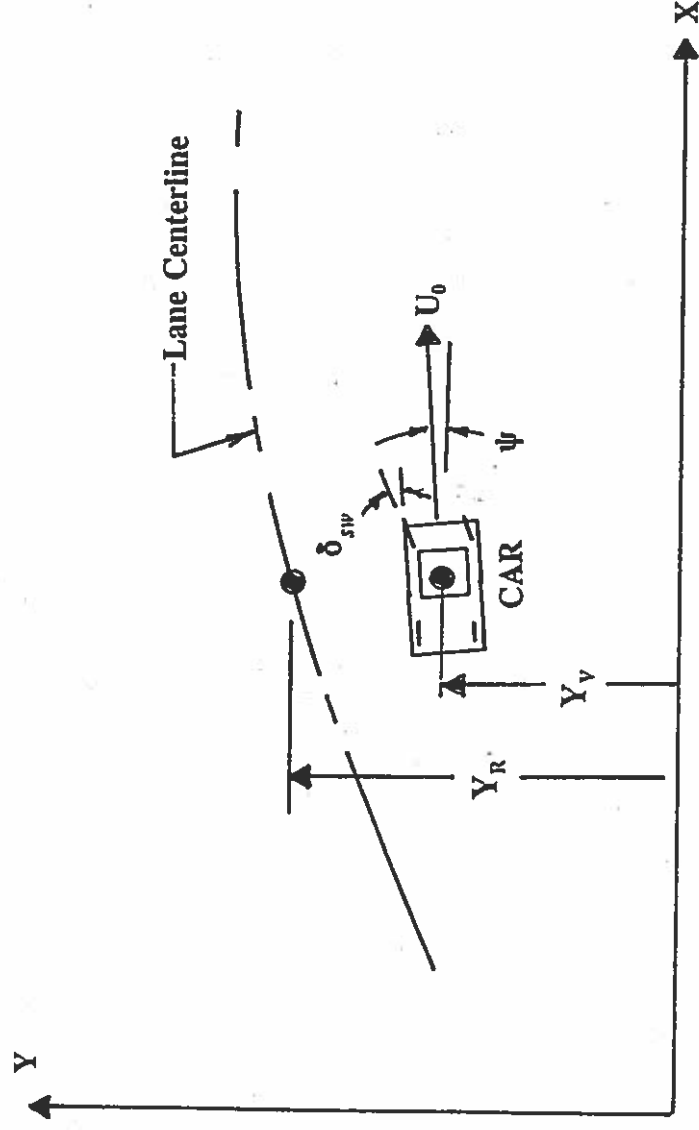


Exercising the Model

Modeling the Automobile Driver

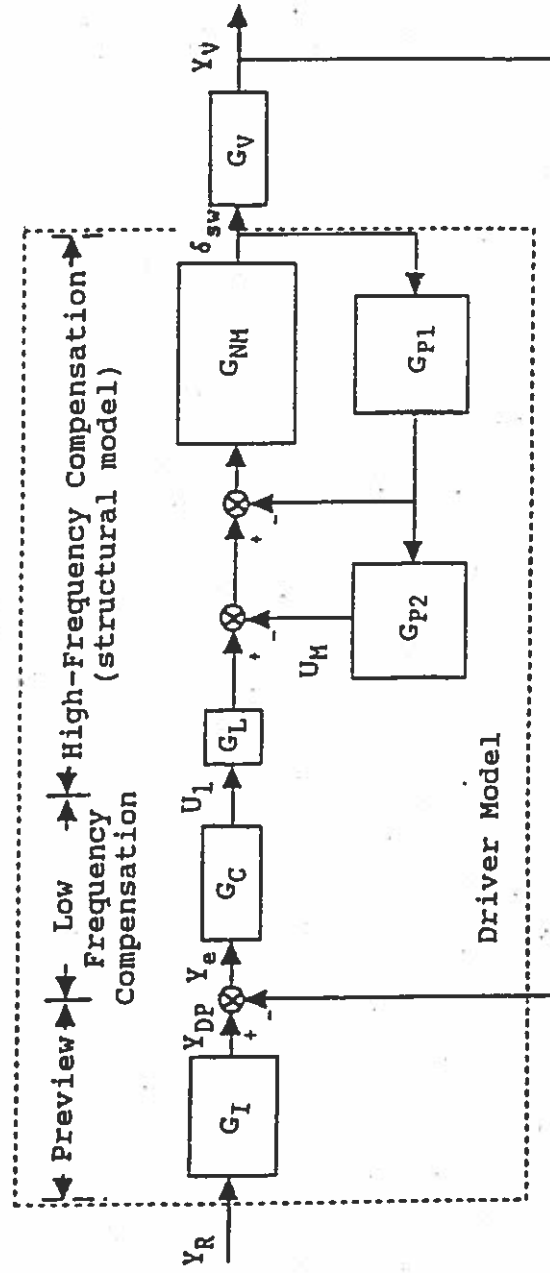
Simplified Driving Task Geometry

Following a Curved Roadway



Modeling the Automobile Driver

An early version of the Structural Model



$$G_I = \frac{e^{-\tau_0 s}}{T_1 s + 1}$$

$$G_L = e^{-\tau_0 s}$$

$$G_{P2} = \frac{K_2}{(s + \frac{1}{T_2})^{k-1}}$$

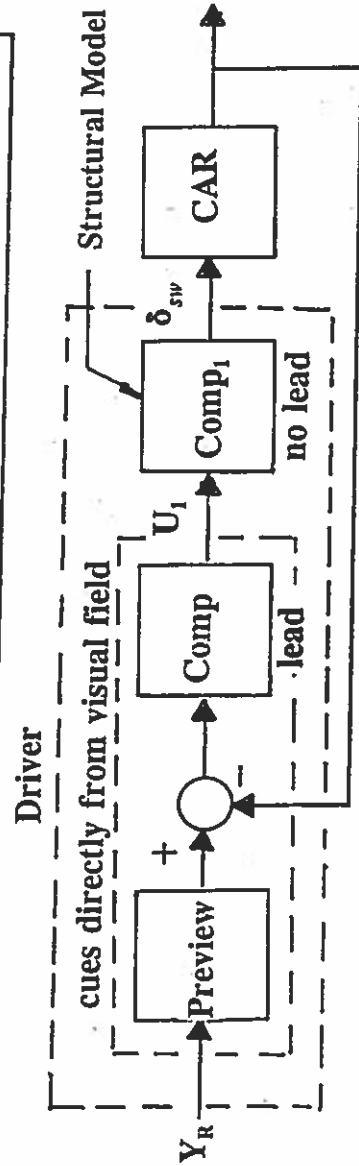
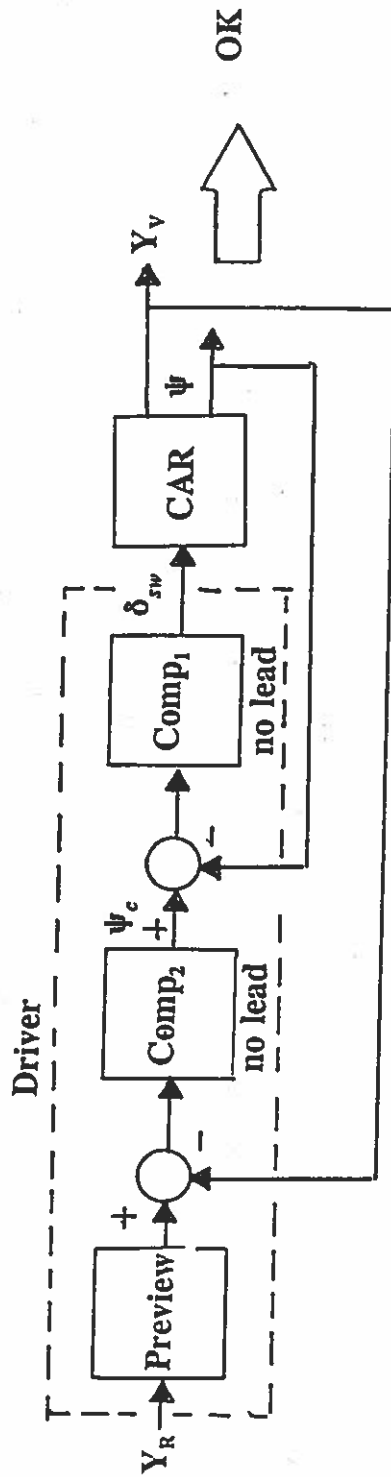
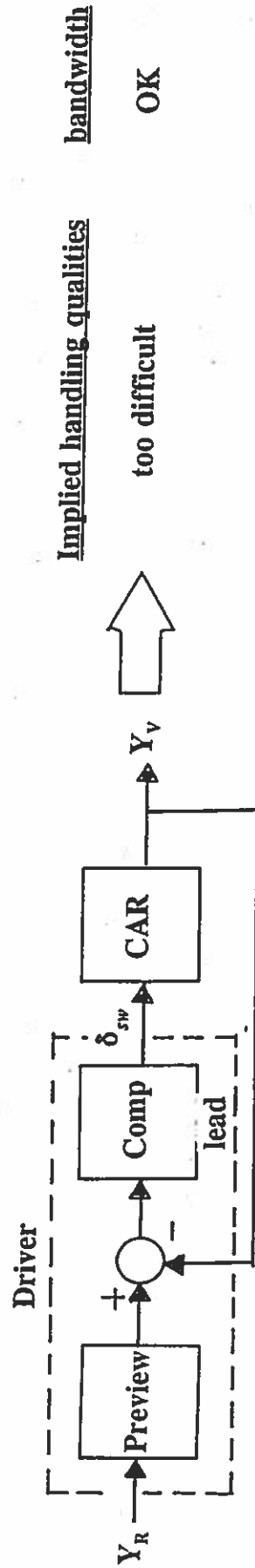
$$G_C = K_y (T_3 s + 1)$$

$$G_{NH} = \frac{\omega_n^2}{(s^2 + 2\zeta_n \omega_n s + \omega_n^2)}$$

$$G_{P1} = \frac{K_1 s}{s + \frac{1}{T_1}}$$

Exercising the Model

Modeling the Automobile Driver



Exercising the Model Modeling the Automobile Driver

Matching Driver Simulation Data Obstacle Avoidance Maneuver

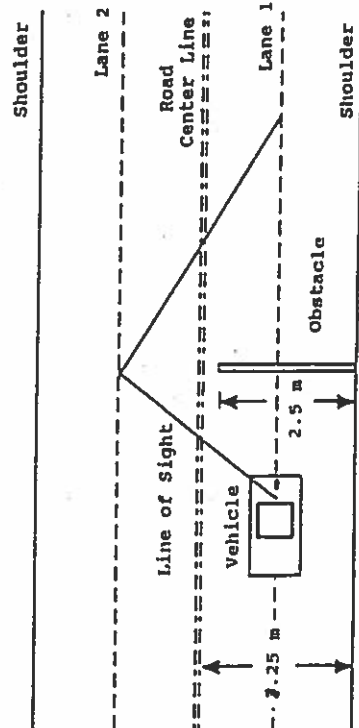
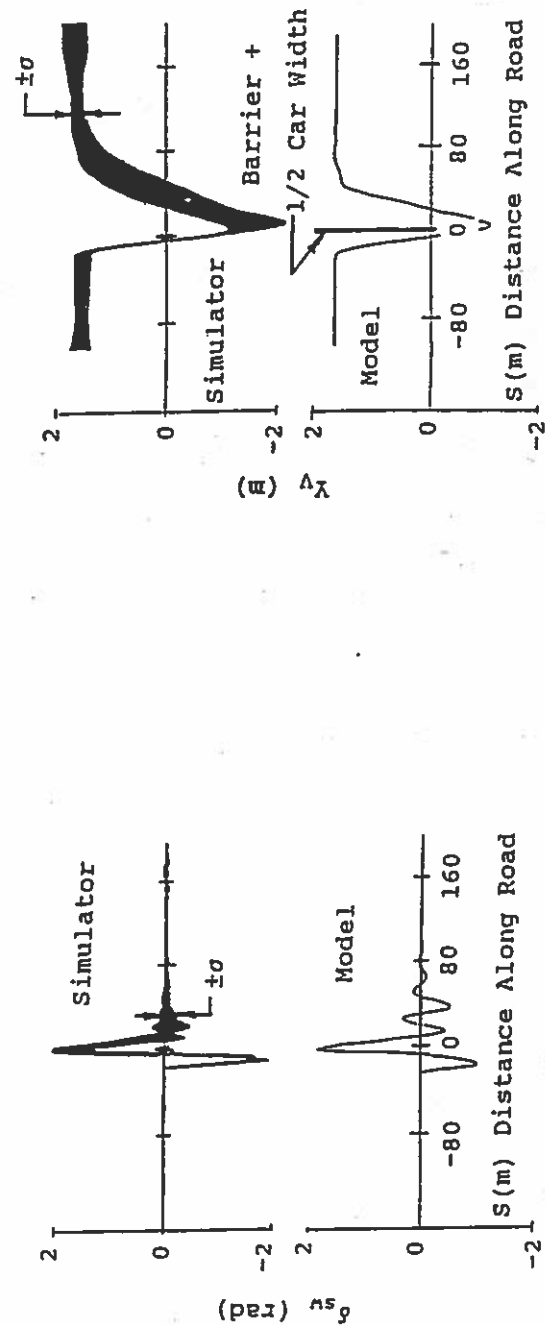


Fig. 10 Geometry for obstacle avoidance task

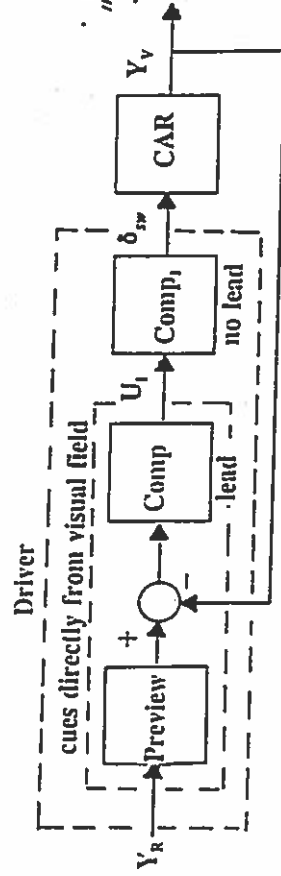


Steering input comparison for obstacle avoidance task

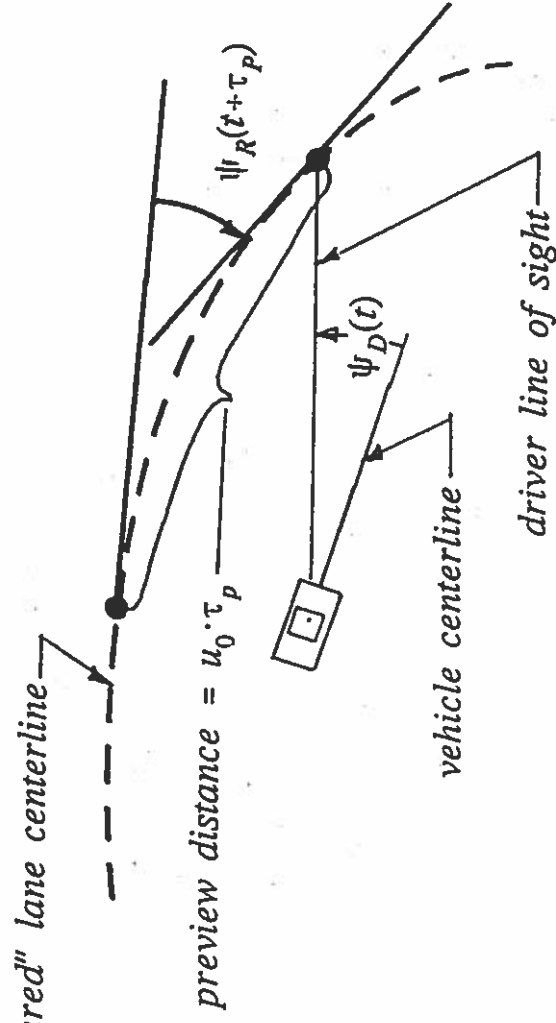
Lateral position comparison for obstacle avoidance task

Exercising the Model Modeling the Automobile Driver

Estimating Visual Field Cues for
Driving on Curvilinear Roadways



$$u_1(t) \approx K_D [\psi_R(t + \tau_p) - \psi_D(t)]$$



Summary

In well-defined flight control tasks, the human pilot adopts a “transfer function” in each control loop that is very similar to that which would be specified by a control system designer to achieve the same closed-loop stability and performance. The primary differences between the inanimate and human controllers are:

- (1) The existence of a time delay on the order of 0.35 sec in the human transfer function
- (2) The inability of the human to higher than first-order lead...i.e., to create a transfer function of the form:

$$K(T_L s + 1)^n e^{-\tau s}$$

where $n > 1$

- (3) The crossover model of the human pilot can be used to estimate the human transfer function
- (4) Reference: Hess, R. A., “Feedback Control Models - Manual Control and Tracking,” Handbook of Human Factors and Ergonomics, 2nd Ed. Wiley, 1997